


## Article

# Fabrication of New TiO<sub>2</sub> Photocatalyst for Removing Organic Dyes and Hazardous VOCs in Air Purifier System

Ji Won Lee <sup>1,2</sup>, Rak Hyun Jeong <sup>1,2</sup>, Ikjo Shin <sup>3</sup> and Jin-Hyo Boo <sup>1,2,\*</sup> 

<sup>1</sup> Department of Chemistry, Sungkyunkwan University, Suwon 16419, Republic of Korea; ljw9917@naver.com (J.W.L.); jrh1015@naver.com (R.H.J.)

<sup>2</sup> Institute of Basic Science, Sungkyunkwan University, Suwon 16419, Republic of Korea

<sup>3</sup> Dokyeung21 Co., Ltd., Suwon 13631, Republic of Korea; ikjoshin@hanmail.net

\* Correspondence: jhboo@skku.edu; Tel.: +82-31-290-7072

**Abstract:** We synthesized an amorphous Ti-based hydroperoxo complex (ATPC) using a facile method involving only titanium hydride (TiH<sub>2</sub>) and H<sub>2</sub>O<sub>2</sub> under mild conditions. We chose TiH<sub>2</sub> as the precursor because it has more reactive sites than metal oxides such as TiO<sub>2</sub>. Qualitative and quantitative optical measurements showed that our synthesized ATPC photocatalysts contained many hydroperoxo groups and various oxidation states of Ti (Ti<sup>2+</sup>, Ti<sup>3+</sup>, and Ti<sup>4+</sup>). Thus, the synthesized ATPC exhibits excellent photocatalytic properties with very fast rates of organic decolorization compared to other conventional visiblelight catalysts. The presence of many hydroperoxo complexes increases the formation of active radicals, which can degrade VOCs such as acetaldehyde in a gas phase. To test the application of the synthesized ATPC, we fabricated a filter system in an air purifier using ATPC coating layers and successfully removed the VOCs. We also proposed a possible photocatalytic oxidation mechanism with ATPC based on this study. It is important to conduct application tests as well as commercialization in photocatalytic experiments.

**Keywords:** visiblelight photocatalyst; Ti-based hydroperoxo complex; coating layer; organic dye and hazardous VOC; air purifier system



**Citation:** Lee, J.W.; Jeong, R.H.; Shin, I.; Boo, J.-H. Fabrication of New TiO<sub>2</sub> Photocatalyst for Removing Organic Dyes and Hazardous VOCs in Air Purifier System. *Catalysts* **2023**, *13*, 935. <https://doi.org/10.3390/catal13060935>

Academic Editors: Leonarda Liotta, Narendra Kumar and Konstantin Ivanov Hadjiivanov

Received: 3 May 2023

Revised: 22 May 2023

Accepted: 24 May 2023

Published: 25 May 2023



**Copyright:** © 2023 by the authors. Licensee MDPI, Basel, Switzerland. This article is an open access article distributed under the terms and conditions of the Creative Commons Attribution (CC BY) license (<https://creativecommons.org/licenses/by/4.0/>).

## 1. Introduction

Recently, industrialization-oriented societies and the reckless use of chemical fuels have caused various environmental problems such as air and water pollution. To solve these issues, ecofriendly studies are being conducted. Among many environmental problems, air pollutants contained in industrial and car emissions, which are the major cause of global warming, are being addressed first. Volatile organic compounds (VOCs) are one of the representative air pollutants that are harmful to both human health and the environment [1,2]. VOCs are harmful compounds and can also cause photochemical reactions with other air pollutants, producing secondary pollutants such as ozone [3,4]. Formaldehyde, acetaldehyde (ACT), and benzene, for example, can cause headaches, vomiting, and dizziness if they come into contact with the skin or enter the respiratory tract [5,6]. These environmental problems need to be urgently resolved because they can cause damage to the nervous system when exposed to high concentrations. Recently, many studies have been conducted to effectively and rapidly remove VOCs, such as adsorption, thermal oxidation, photocatalytic oxidation, and biofiltration [7–9]. Among them, photocatalysts have been widely studied because they are environmentally friendly and produce water (H<sub>2</sub>O) and carbon dioxide (CO<sub>2</sub>) as final byproducts [10–12]. In addition, photocatalytic materials have the advantage of being activated with only solar energy. Resolving energy shortages and environmental pollution problems has become the most urgent challenge nowadays. Using a catalyst as one of the many solutions can lower the activation energy of the reaction, producing more energy for us to use. Among the various catalysts, photocatalysts, which are more environmentally friendly and utilize light sources, have been extensively studied.

There are three main reasons why many studies on photocatalysts have been conducted. First, photocatalysts can be active even at room temperature, unlike other catalysts that require high temperatures. Second, the photocatalytic reaction can be induced by utilizing sunlight, which is an infinite resource. Third, the photocatalytic reaction can be stopped at a desired point in time by blocking the supply of sunlight. Therefore, photocatalysts can play an important role in solving future environmental issues such as energy conservation and global warming.

Titanium dioxide ( $\text{TiO}_2$ ) is a well-known semiconductor material and is widely used as a photocatalytic material owing to its strong oxidizing power and excellent durability [13].  $\text{TiO}_2$  is also utilized for solar energy conversion applications such as solar cells by utilizing its inherent bandgap [14]. However,  $\text{TiO}_2$  has a bandgap of  $\sim 3.0\text{--}3.2$  eV, which only allows it to absorb UV light, making bandgap engineering necessary for the effective utilization of light sources. The development of a photocatalyst with visible light activity is crucial as most of the sunlight energy is in the visible light region. Many studies have been performed to overcome this problem, and a typical method of bandgap engineering is achieved by either metal doping or nonmetal doping to  $\text{TiO}_2$  [15] as well as by coupling with a semiconductor with a narrow bandgap [16]. Although such photocatalytic materials have visible light activities, they also have several disadvantages. For example, the process of making narrow bandgaps by doping or coupling is complicated and requires high temperature and pressure [17], and these materials have low photocatalytic efficiency in visible light. Recently, extensive effort has been devoted to forming peroxo groups ( $\text{Ti-OOH}$ ,  $\text{--Ti-O-O-Ti--}$ , and  $\text{--O-Ti-O--}$ ) by oxidizing metal oxide surfaces with  $\text{H}_2\text{O}_2$  [18]. The hydroperoxo photocatalysts have visible light activity and can cause electron transfer into the conduction band (CB) of metal oxide, forming a superoxide anion. Generating metal oxides with a peroxo (or hydroperoxo) surface is a relatively simple process, and such metal oxides with a hydroperoxo surface have excellent visible light photocatalytic efficiency that can be applied to various fields. Therefore, another study was conducted to synthesize photocatalysts that have visible light activity by intentionally creating oxygen vacancies in the  $\text{TiO}_2$  lattice. For example, hydrogenated  $\text{TiO}_2$  with an oxygen vacancy can be synthesized by adding a strong reducing agent such as  $\text{NaBH}_4$  to  $\text{TiO}_2$  [19]. Studies have also been conducted on the synthesis of  $\text{Ti}^{3+}$  self-doped  $\text{TiO}_2$  through the hydrothermal method using  $\text{TiCl}_3$  and  $(\text{NH}_4)_2\text{TiF}_6$  as the precursor of  $\text{Ti}^{3+}$  and  $\text{Ti}^{4+}$ , respectively [20]. These photocatalysts achieve visible light activity owing to the oxygen defects in the synthesized titania-based photocatalysts, ultimately allowing the absorption of visible light by forming a new donor level in the band structure.

Herein, we synthesized an amorphous Ti-based hydroperoxo complex (ATPC) using only titanium hydride (metallic Ti) and  $\text{H}_2\text{O}_2$  under mild conditions through a facile method. Polymerization was used to generate the ATPC without annealing through an exothermic reaction. To investigate how the peroxo groups and oxygen vacancy of ATPC affect the visible light catalyst, the decolorization of Rhodamine B (RhB) dye was performed under visible light irradiation. Next, we tested the ability of the ATPC to remove acetaldehyde (ACT), one of the VOCs in the gas phase. Finally, we tested the application of ATPC as a filter system in an air purifier.

## 2. Results and Discussion

### 2.1. Photocatalytic Activity Test with Amorphous Ti-Based Hydroperoxo Complex (ATPC)

To test the photocatalytic activity of the synthesized ATPC, we dissolved the ATPC powder in water and performed spin coating on a glass substrate. Two samples were prepared with different coating numbers to determine the thickness of the thin film showing appropriate catalytic characteristics. Figure 1c,d showed that a one-time coated layer yielded a thin film with a thickness of  $\sim 180$  nm, while a two-time coated layer yielded a thin film with  $\sim 320$  nm thickness. The surface shown in Figure 1b is rougher than that shown in Figure 1a, indicating different surface area. To measure the specific surface area of two different films, BET analysis was performed with a nitrogen gas adsorption–desorption

isotherm. The thin films with thickness of 180 and 320 nm had the specific surface area of 129.9 and 166.5 m<sup>2</sup>/g, respectively. This suggests that thicker film will show more high catalytic activity than thinner film owing to a larger surface area. Therefore, the surface area strongly depends on the coating number. However, in our case if the film was thicker than 320 nm, the catalytic activity decreased, indicating that the catalytic reaction mainly occurred on the surface region rather than in the bulk area. Therefore, an optimized thickness of a photocatalyst is required to obtain the maximum catalytic activity.

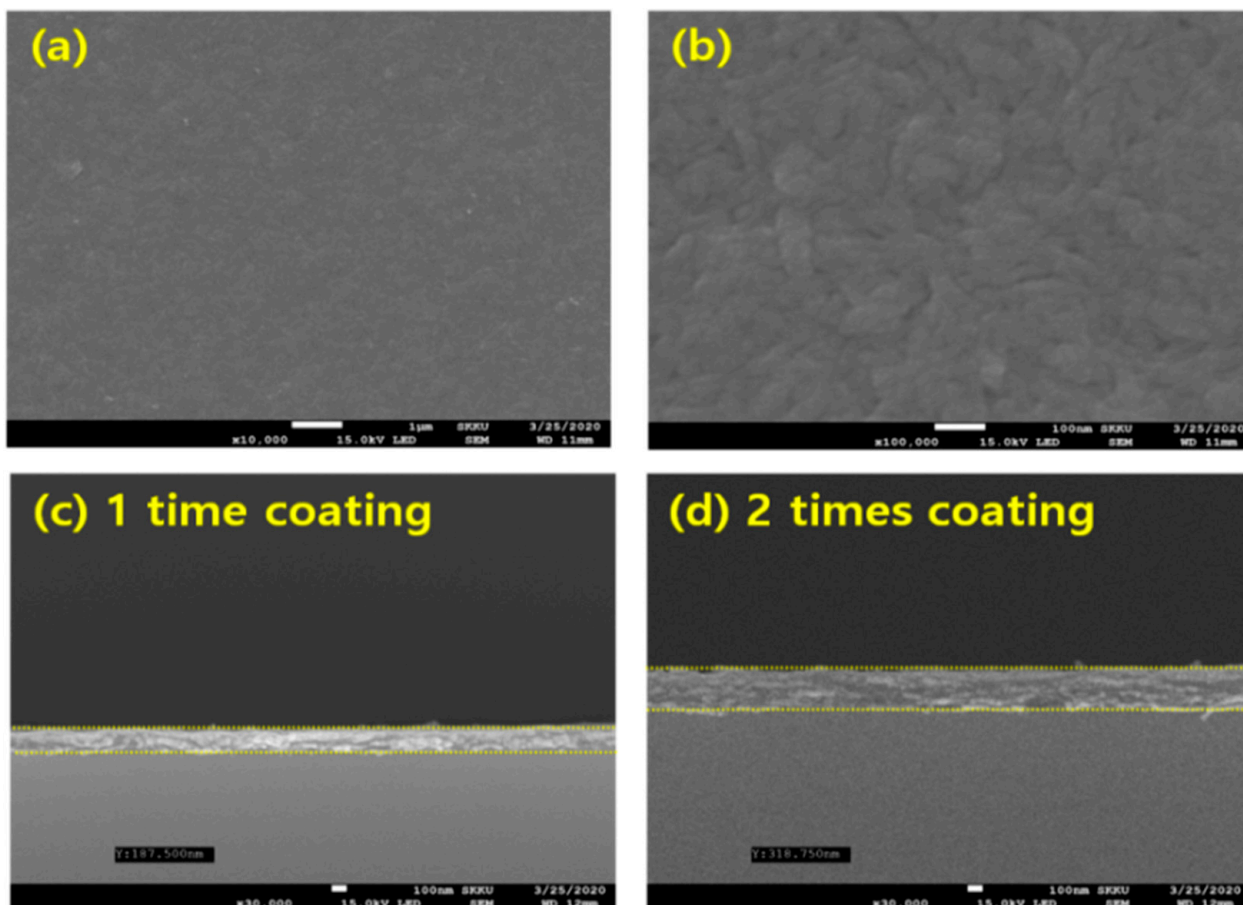


**Figure 1.** FE-SEM images of (a) one-time ATPC coated sample and (b) two-time ATPC coated sample. (c,d) show their cross-sectional images, respectively.

We performed the decolorization of the RhB dye under visible light irradiation to confirm how the peroxo group and oxygen vacancy of ATPC surface affected the visible light catalyst (see also Section 3). Our synthesized ATPC photocatalysts showed very fast organic decolorization rates owing to the formation of many active radicals such as OH radicals. We added 20 mg of samples to a concentration of RhB solution and stirred it in a dark room for 30 min to establish an adsorption–desorption equilibrium. We used a 200 W blue LED lamp as the light source, and the total irradiation time of each sample was 2 h. After 2 h, we separated the RhB mixture from the sample using centrifugation and measured the absorbance using a UV–Visible spectrophotometer. Figure 2 shows that the two-time coated sample (Figure 2b) decomposed more RhB dye in the same time than the one-time coated sample (Figure 2a), reflecting thickness and surface area differences as well as peroxo groups on the ATPC surface. We also found that there was no considerable difference when coating two or more times. Therefore, we used the same sample of two-time coating with a thickness of ~320 nm to check the photocatalytic activities for other VOCs such as ACT in a gas phase.

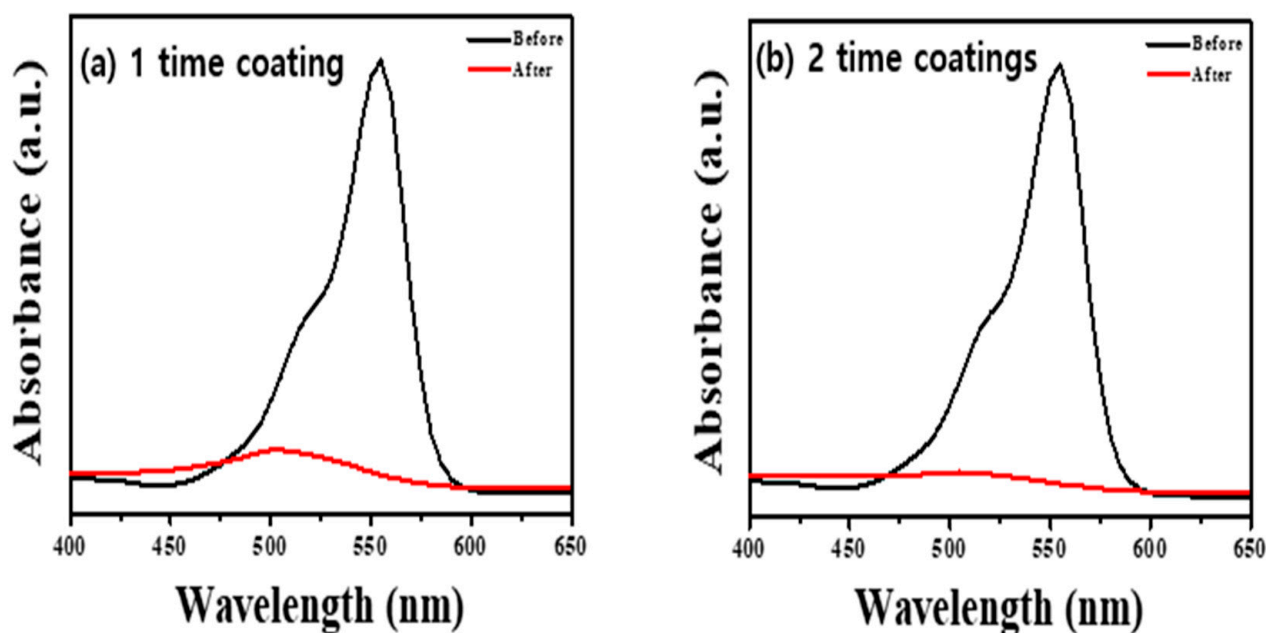


**Figure 2.** UV-Visible absorption spectra obtained before and after decolorization of RhB dye with (a) one-time ATPC coated sample and (b) two-time ATPC coated sample.

The experiment involved the degradation of acetaldehyde (ACT) in a gas phase using a flow-type reactor equipped with an online gas chromatography (GC, HP 6890, HEWLETT PACKARD). The stationary phase and detector of the GC were the HP-PLOT Q column and the flame ionization detector, respectively. The synthesized ATPC powder (500 mg) in a quartz boat was placed at the center of the quartz tube. A gas mixture containing 107.7 ppm of ACT and dry air was flowed into a photocatalytic reactor using mass flow controllers, while blue light (10 W, KWLD B1207W, Kwangwon light) was irradiated on the sample at a distance of ~10 cm. The gas mixture that passed through the sample was injected into the GC every 10 min, and the amount of ACT and CO<sub>2</sub> were monitored with the lightirradiation time. Figure 3a shows that CO<sub>2</sub> is generated as ACT is removed, and it can be seen that ~15% of the ACT can be removed within 5 h. The power (10 W) used was relatively weak compared to 200 W for the decolorization of the RhB dye; hence, more time was required to remove the ACT. A 10 W small powered blue LED was used as the light source to consider its installation inside an air purifier system. Therefore, only 15% of the ACT was removed in 5 h. However, if a stronger power source, such as a 200 W blue LED lamp, was used, the percentage of removal could be increased to >60% within only 2 h, suggesting an increased functionality of photocatalytic activity.

Based on this study, we suggested a possible photocatalytic oxidation mechanism of ATPC as follows [21]. When the hydroperoxo group (Ti-OOH) absorbs visiblelight, radicals are formed and an electron (e<sup>-</sup>) is also formed by combining with an unshared electron pair of oxygen. The formed e<sup>-</sup> reacts with oxygen in the air to form superoxide anions, providing strong oxidation. The remaining plus-charged hydroperoxo groups react with water molecules on the photocatalyst's surface to form OH radicals, which degrade the contaminants (i.e., ACT) through oxidation [21–23]. To prove and clarify these mechanisms utilizing various analytical instruments, we have to carry out both in-situ and ex-situ experiments to detect intermediates, radicals, holes, and electrons by time-resolved photoluminescence (TRPL), time-dependent light irradiated UV-Vis spectra, transient absorption spectroscopy, electron spin resonance (ESR), X-ray photoelectron spectroscopy (XPS), Diffuse Reflectance Fourier Translation Infrared Spectroscopy (DRIFTS), etc. Recently, Shu et al. proposed similar photocatalytic oxidation of ammonia (NH<sub>3</sub>) on TiO<sub>2</sub>-based catalysts such as P25 and nanosheet TF4 [23]. For systematic investigation into the NH<sub>3</sub> adsorption and conversion behaviors, they utilized in-situ DRIFTS and

obtained a progressed mechanism of  $\text{NH}_3$  photocatalytic oxidation. Additionally, Karmakar et al. proposed the  $\text{CO}_2$  photocatalytic reduction mechanism based on time-dependent in-situ DRIFTS experiments on  $\text{CO}_2$  reduction in a mixture of  $\text{CO}_2$  and  $\text{H}_2\text{O}$  vapor on Ce-MOF-RuII-bpy surface [24]. Based on our data and suggested mechanisms, therefore, our ATPC photocatalytic efficiency shows the best performance because it can form more electrons than conventional photocatalytic  $\text{TiO}_2$  materials. For these reasons, as seen in Figure 3b, the adsorption and degradation of ACT proceeded rapidly on the surface of ATPC particles. Air pollutants such as ACT are initially adsorbed on the surface of the ATPC photocatalyst, and subsequently photo-oxidative decomposition occurs through light-induced electron-hole pairs. After the reaction, the finally formed water ( $\text{H}_2\text{O}$ ) and carbon dioxide ( $\text{CO}_2$ ) are desorbed from the adsorption site of the ATPC photocatalyst surface.

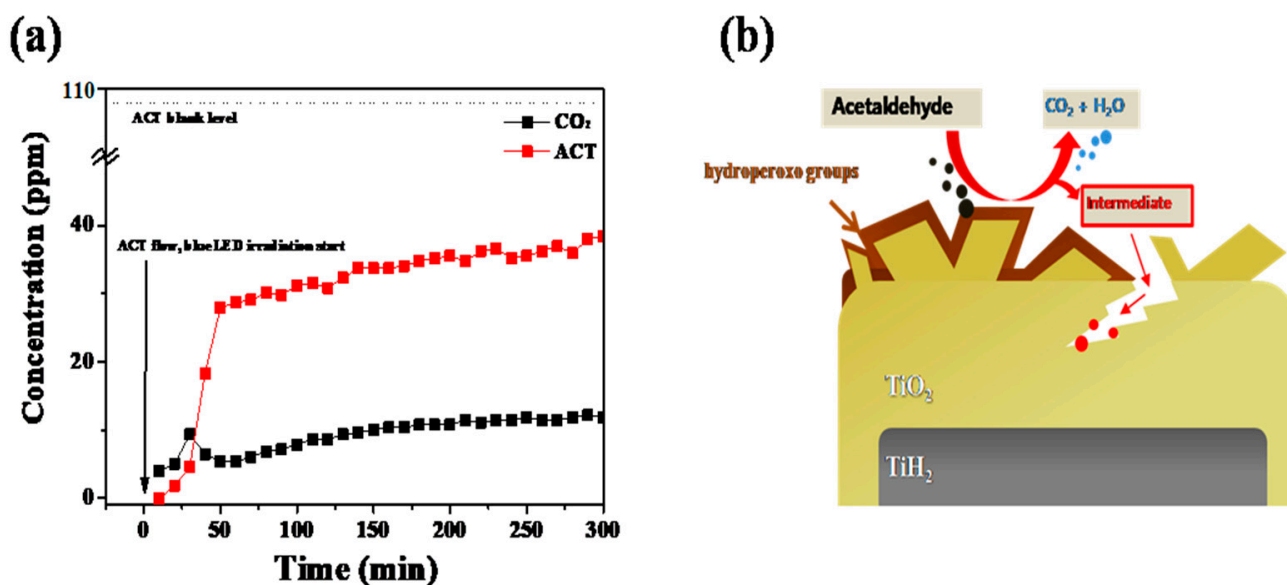
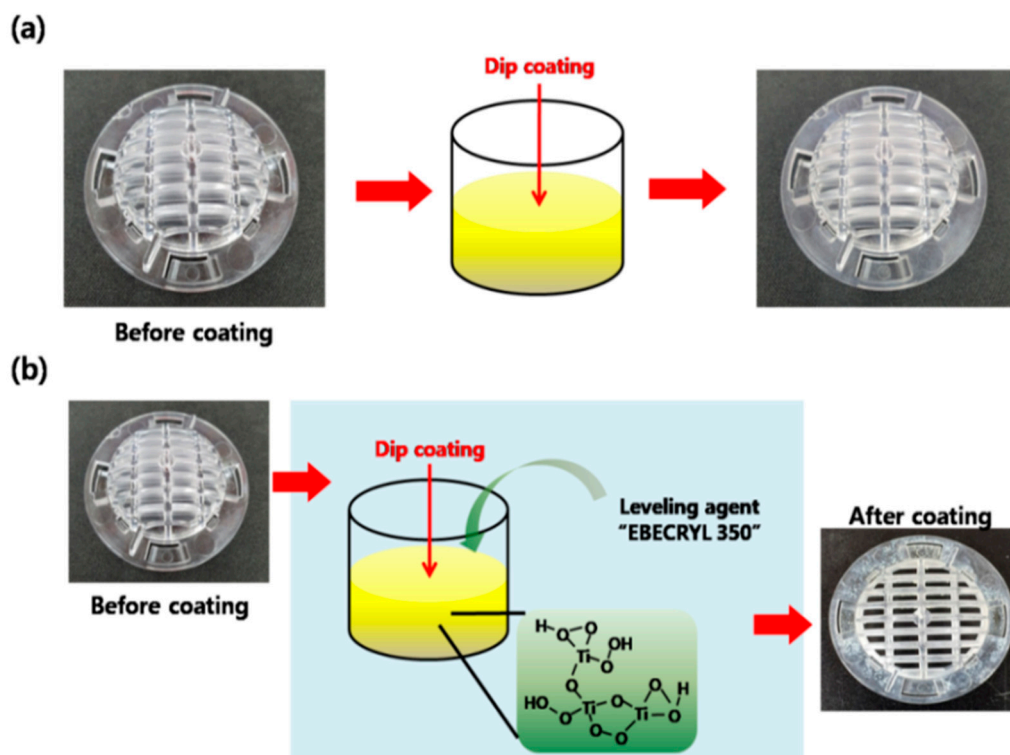


Figure 3. (a) Photocatalytic degradation test of acetaldehyde with two-time ATPC coated sample, and (b) photocatalytic oxidation mechanism of ACT on ATPC surface.

## 2.2. Application Test for Air Purifier System

As people spend more time indoors, there is a growing interest in creating a comfortable and healthy indoor air environment. This has led to increased research into ecofriendly airpurification mechanisms [25,26]. Based on the ecofriendly characteristics of our ATPC samples, they have potential for use in future applications that prioritize efficiency and durability. We successfully incorporated our synthesized ATPC coating layers into a filter system in an air purifier and were able to effectively remove VOCs. To test the commercial viability of our photocatalyst, we applied it to the filter of a small car air purifier. Figure 4 provides a schematic of two different coating methods: (a) direct dip coating of the photocatalyst onto the ABS plastic filter substrate, and (b) dip coating with the addition of the adhesion-promoting leveling agent, EBECRYL 350 (EB-350), to improve the bond between the coating layer and the ABS plastic substrate surface. As shown in Figure 5a, it was very tough for us to obtain a uniform and thick ATPC film on the ABS plastic substrate with good adhesion. Therefore, we introduced an adhesion-promoting leveling agent, EBECRYL 350 (EB-350), to improve the adhesion between the coating layer and the plastic substrate surface. With EB-350, we could modify the plastic surface first, and then successfully grow uniform and thick ATPC film on the ABS plastic substrate, resulting in good adhesion and high photocatalytic activity.





**Figure 4.** Schematic for dip coatings of the APTC layer on the ABS plastic filter substrates (a) without EB-350 and (b) with EB-350.

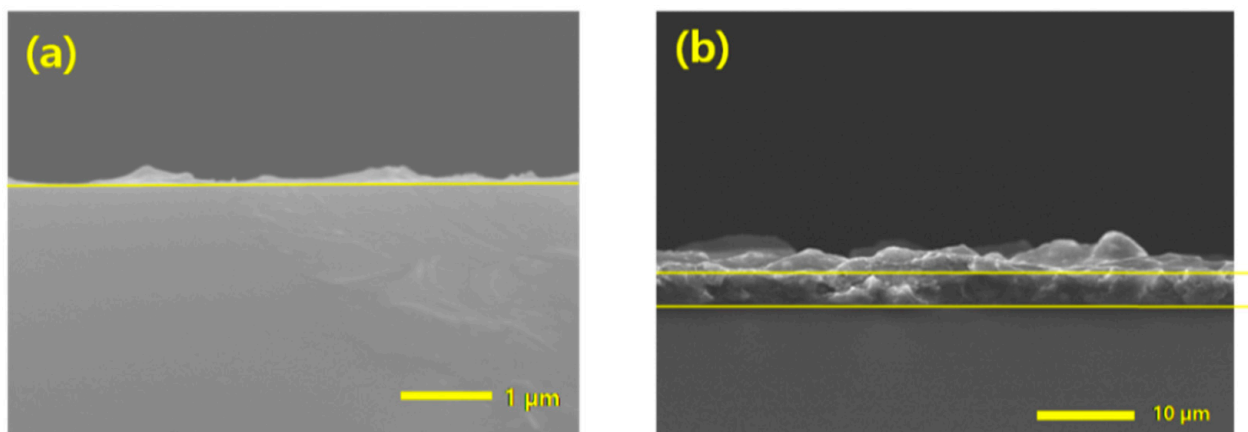


**Figure 5.** SEM cross-sectional images of the APTC coating layers on the ABS plastic filter substrates (a) without EB-350 and (b) with EB-350.

The cross-sectional images of the coatings are presented in Figure 5. Figure 5a shows the rough surface and thin film thickness of the photocatalyst coated by dip coating without EB-350, while Figure 5b shows a relatively uniform surface and a greater film thickness with the addition of EB-350. A coating film was obtained in Figure 5b that exhibited photocatalytic performance similar to that obtained by spin coating twice on a glass substrate.

Figure 6 displays the results of the RhB removal experiment using the coatings shown in Figure 5. In Figure 6a, only ~40% of the RhB was removed in 2 h owing to the very small thickness and poor surface uniformity, whereas in Figure 6b, >90% of the RhB was removed in 2 h due to a thick film with a high surface area and good uniformity, as well as better adhesion between the APTC coating layer and the substrate. These results demonstrate

that our synthesized ATPC photocatalyst can be used commercially and can be adopted as an airpurifier filter to remove more VOCs in the future.

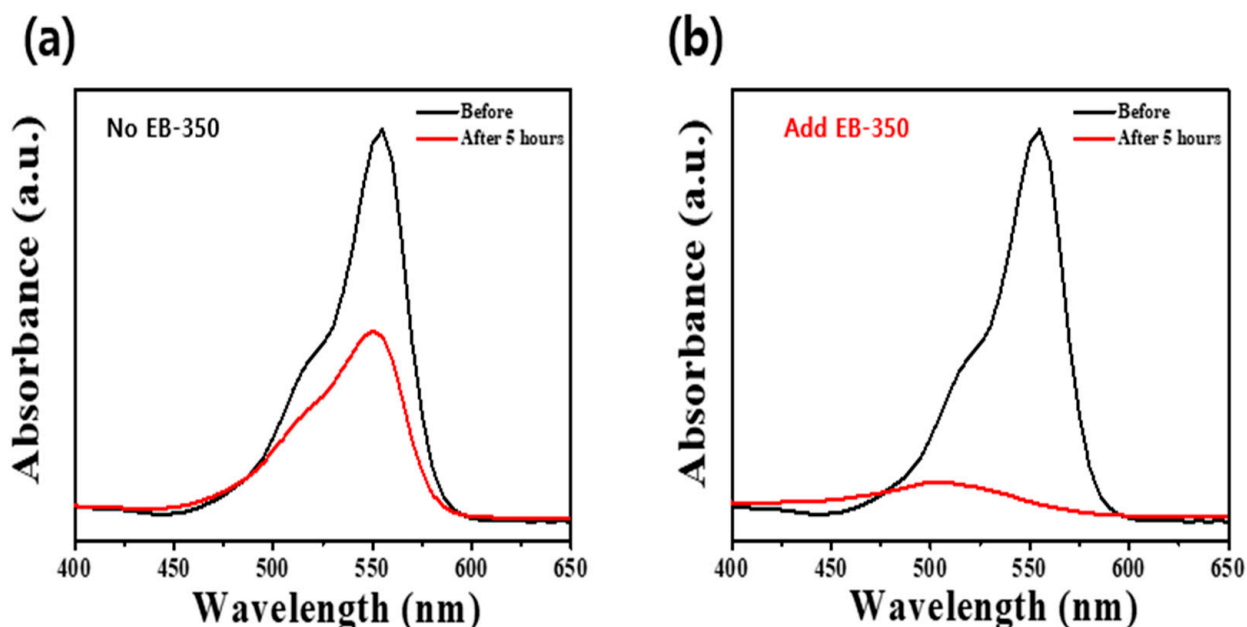


**Figure 6.** UV–Visible absorption spectra obtained before and after decolorization of RhB dye with the ATPC coating layers on the ABS plastic filter substrates (a) without EB-350 and (b) with EB-350.

Figure 7 depicts the appearance of an air purifier with the filter of Figure 4b installed inside a vehicle. The product is expected to be released and sold as early as next year in gold and silver colors. We will also consider more colors and designs that reflect flow mechanics for future products to cater to the consumer’s preference.



**Figure 7.** Images of air purifier adapted ATPC filter.

### 3. Materials and Methods

#### 3.1. Synthesis of Amorphous Ti-Based Hydroperoxo Complex (ATPC)

All the chemicals used in the synthesis of the amorphous Ti-based hydroperoxo complex (ATPC), namely titanium hydride ( $\text{TiH}_2$ , Sigma-Aldrich, St Louis, MO, USA) and

hydrogen peroxide solution ( $\text{H}_2\text{O}_2$ , 30 wt.% in  $\text{H}_2\text{O}$ , Sigma-Aldrich), were used as starting agents without any further purification. The typical synthetic method for ATPC was very simple. First,  $\text{TiH}_2$  powder (3.0 g) and distilled water (75 mL) were vigorously stirred at 25 °C. Second, 100 mL of  $\text{H}_2\text{O}_2$  was slowly added into the solution to form a  $\text{Ti-OOH}$  surface with a  $\text{TiH}_2$  core. After 1.5 h, metallic Ti reacted with  $\text{H}_2\text{O}_2$ , resulting in a gray colored gel state due to an exothermic reaction, followed by an increase in temperature up to 100 °C. Finally, 50 mL of  $\text{H}_2\text{O}_2$  was added into the gray gel and stirred for 1 h to form a green colored gel state. After the gel was dried at 100 °C and ground, a fine powder was obtained. The details of our synthetic method as well as the characteristics of ATPC have already been reported elsewhere [21]. With the measurements of XPS and Raman spectra, we confirmed that our synthesized ATPC photocatalysts had large amounts of hydroperoxo groups and many oxygen vacancies on the ATPC surface that could induce very high photocatalytic activity under the visible light catalyst.

XPS shown in Figure 8 was measured to confirm the Ti oxidation number and oxygen related species as well as oxygen vacancy. As shown in the bottom figure of Figure 8a, the typical binding energy of  $\text{Ti}^{4+}$  was confirmed in the case of  $\text{TiO}_2$ . One noticeable thing is that the binding energy of metallic Ti and  $\text{Ti}^{4+}$  was confirmed through the data of  $\text{TiH}_2$ , because the surface of  $\text{TiH}_2$  can easily oxidize even in the air. In the case of green and yellow colored ATPC, they showed the various Ti oxidation states such as  $\text{Ti}^{2+}$ ,  $\text{Ti}^{3+}$ , and  $\text{Ti}^{4+}$ . This was because surface oxidation proceeded slowly from metallic Ti. In addition, Figure 8b shows the measurements of the O 1s peaks and the results are as follows. First, the green colored ATPC showed the oxygen-bonded binding energy between  $\text{Ti}^{4+}/\text{Ti}^{2+}$  and  $\text{V}_\text{O}$  (oxygen vacancy)/ $\text{TiOH}/\text{TiOOH}$  observed to be high. This could be attributed to our synthesized peroxy complexes, as oxidation and polymerization reactions took place on  $\text{TiH}_2$  surface. In the case of yellow colored ATPC, it can be explained that the oxidation reaction proceeded by  $\text{H}_2\text{O}_2$  from the green gel so that the  $\text{Ti-OOH}$  groups increased. Raman spectra were also measured to obtain supplement information for peroxy groups present in the synthesized ATPC. As shown in Figure 8c, there were two vibration modes (916 and 685  $\text{cm}^{-1}$ ) originating from the peroxy groups. In addition, strong  $\text{E}_\text{g}$  mode (286  $\text{cm}^{-1}$ ) derived from oxygen vacancy and typical  $\text{TiO}_2$  vibration mode (531  $\text{cm}^{-1}$ ) was also measured [27].

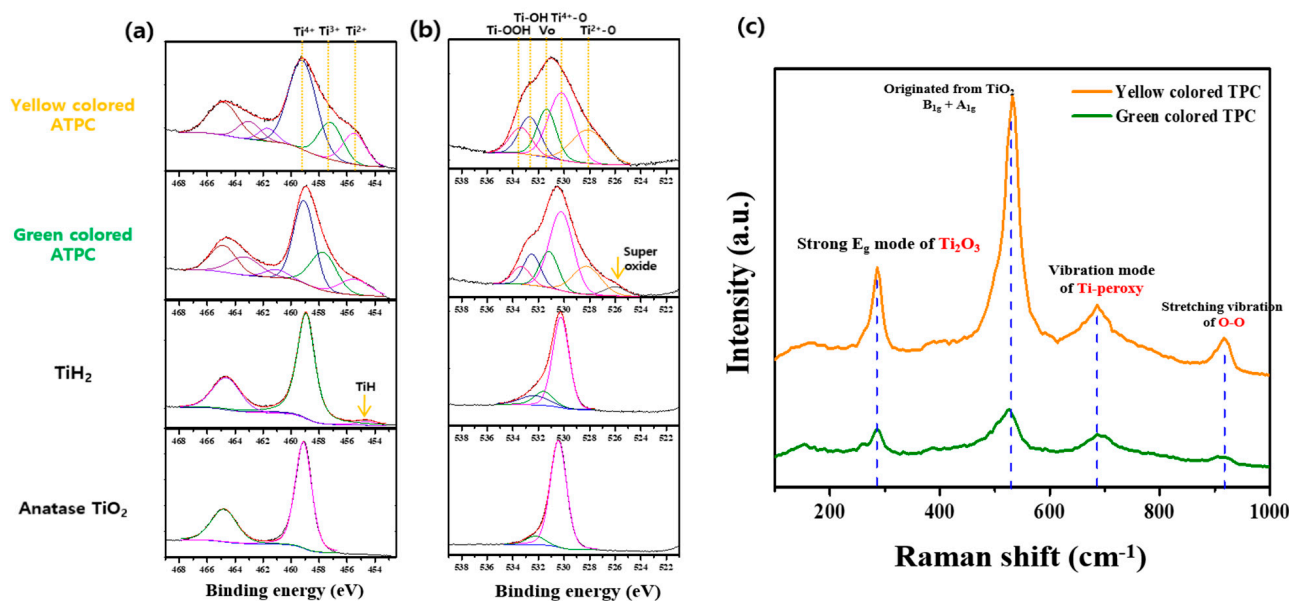


**Figure 8.** X-ray photoelectron spectra of (a) Ti 2p level and (b) O 1s level of anatase  $\text{TiO}_2$ ,  $\text{TiH}_2$ , green and yellow colored ATPC. (c) shows the Raman spectra of green and yellow colored ATPC.



### 3.2. Characterization

Under a 200 W blue LED lamp, the photocatalytic activity of the synthesized ATPC was first evaluated by the decolorization of RhB. Figure 9 presents the detailed diagrams for the photocatalytic activity measurements for the removals of (a) RhB dye and (b) ACT VOC, respectively. In a typical photocatalytic activity measurement procedure, 20 mg of ATPC powder was added to a 70 mL aqueous solution of 10 ppm RhB and stirred for about 30 min to establish an adsorption–desorption equilibrium. As the first step, a blank test was conducted for about 30 min to confirm whether the RhB dye was physically adsorbed on the surface of the ATPC photocatalyst or decomposed without a visible light source. Next, under visible light conditions, the suspensions were irradiated at a certain distance. During light irradiation, every 5 min the suspensions (each 4 mL) were collected and separated via centrifugation. The separated solution was transferred to a 1 cm × 1 cm cuvette for absorbance measurement using a UV–Visible spectrophotometer. By checking the peak of absorbance at 550 nm corresponding to the  $\pi \rightarrow \pi^*$  transition, the photocatalytic activities of each sample were measured. An application test for an airpurifier system was also conducted with the synthesized ATPC coating layers as follows. First, the samples were washed and centrifuged with distilled water after each photocatalytic activity measurement was finished to remove the RhB dye from the sample surface. The following procedure was repeated several times.

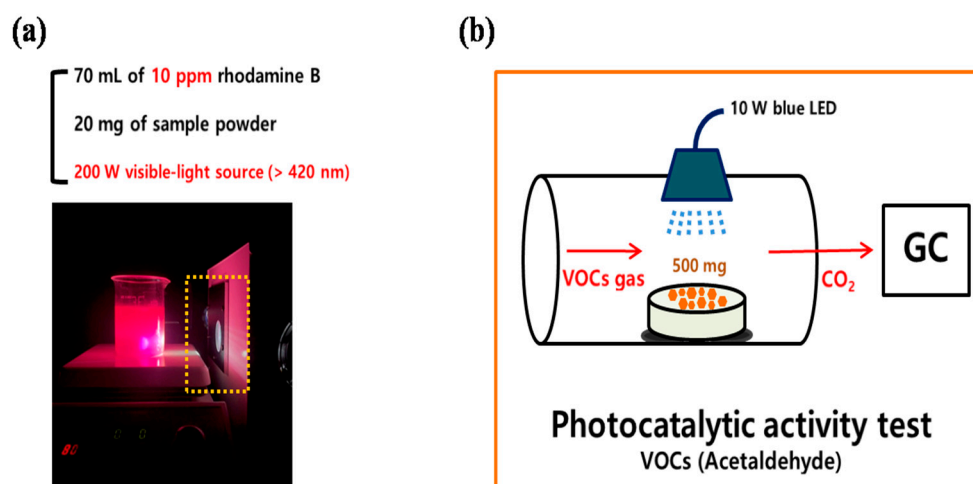


**Figure 9.** Schematic of the photocatalytic activity tests for the removal of (a) RhB dye and (b) ACT VOC.

### 4. Conclusions

In this study, an amorphous Ti-based hydroperoxo complex (ATPC) as the new photocatalyst involving only titanium hydride (TiH<sub>2</sub>) and H<sub>2</sub>O<sub>2</sub> was synthesized by using a facile method under mild conditions. Based on the results presented above, we conclude that all the synthesized samples showed a good degradation efficiency owing to the active carriers formed from the peroxo groups and oxygen vacancies of ATPC. Overall data suggest that this study presents a very good approach to solving air pollution problems such as VOCs. The reason is that in the process of synthesizing ATPC, not only low-cost precursors were used but also a facile synthesis method at room temperature was proposed. Moreover, both the synthesis of ATPS and the fabrication of ATPC-based coating layer are expected to be applicable to various fields such as the removal of both organic pollutants and hazardous wastes as well as a scale-up synthesis method. In addition, since our synthetic method does not need any additional heat or pressure during the synthesis process, this mild synthetic method will be very valuable if it can be applied to other metallic materials besides TiH<sub>2</sub>. Furthermore, it will be easy to build a mass synthesis system in an industrial aspect later.

**Author Contributions:** Conceptualization, J.W.L. and J.-H.B.; methodology, J.W.L.; software, R.H.J.; validation, J.W.L., R.H.J. and I.S.; formal analysis, J.W.L.; investigation, J.W.L.; resources, J.-H.B.; data curation, R.H.J.; writing—original draft preparation, J.W.L.; writing—review and editing, R.H.J., I.S. and J.-H.B.; visualization, J.W.L.; supervision, J.-H.B.; project administration, J.-H.B.; funding acquisition, J.-H.B. All authors have read and agreed to the published version of the manuscript.

**Funding:** This work was supported by Basic Science Research Program through the National Research Found This ation of Korea (NRF) funded by the Ministry of Education (No. NRF-2019R1A6A1A10073079).

**Data Availability Statement:** Not applicable.

**Conflicts of Interest:** The authors declare no conflict of interest.

## References

- Liu, Y.; Shao, M.; Fu, L.; Lu, S. Source profiles of volatile organic compounds (VOCs) measured in China: Part I. *Atmos. Environ.* **2008**, *42*, 6247–6260. [\[CrossRef\]](#)
- Phillips, M.; Herrera, J.; Krishnan, S. Variation in volatile organic compounds in the breath of normal humans. *J. Chromatogr. B* **1999**, *729*, 75–88. [\[CrossRef\]](#)
- Fan, Z.; Li, P.; Weschler, C.; Fiedler, N.; Zhang, J. Ozone-Initiated Reactions with Mixtures of Volatile Organic Compounds under Simulated Indoor Conditions. *Environ. Sci. Technol.* **2003**, *37*, 1811–1821. [\[CrossRef\]](#) [\[PubMed\]](#)
- Calfapietra, C.; Fares, S.; Manes, F.; Morani, A.; Sgrigna, G.; Loreto, F. Role of Biogenic Volatile Organic Compounds (BVOC) emitted by urban trees on ozone concentration in cities: A review. *Environ. Pollut.* **2013**, *183*, 71–80. [\[CrossRef\]](#)
- He, J.; Zou, Z.; Yang, X. Measuring whole-body volatile organic compound emission by humans: A pilot study using an air-tight environmental chamber. *Build. Environ.* **2019**, *153*, 101–109. [\[CrossRef\]](#)
- Yang, S.; Gao, K.; Yang, X. Volatile organic compounds (VOCs) formation due to interactions between ozone and skin-oiled clothing: Measurements by extraction-analysis-reaction method. *Build. Environ.* **2016**, *103*, 146–154. [\[CrossRef\]](#)
- Yu, L.; Wang, L.; Xu, W.; Chen, L. Adsorption of VOCs on reduced graphene oxide. *J. Environ. Sci.* **2018**, *67*, 171–178. [\[CrossRef\]](#)
- Kamal, M.S.; Razzak, S.A.; Hossain, M.M. Catalytic oxidation of volatile organic compounds (VOCs)—A review. *Atmos. Environ.* **2016**, *140*, 117–134. [\[CrossRef\]](#)
- Yang, C.; Qian, H.; Li, X.; Cheng, Y.; He, H.; Zeng, G.; Xi, J. Simultaneous Removal of Multicomponent VOCs in Biofilters. *Trends Biotechnol.* **2018**, *36*, 673–685. [\[CrossRef\]](#)
- Ostyn, N.R.; Steele, J.A.; Prins, M.D. Low-temperature activation of carbon black by selective photocatalytic oxidation. *Nanoscale Adv.* **2019**, *1*, 2873–2880. [\[CrossRef\]](#)
- Sheng, Z.; Ma, D.; He, Q.; Wu, K. Mechanism of photocatalytic toluene oxidation with ZnWO<sub>4</sub>: A combined experimental and theoretical investigation. *Catal. Sci. Technol.* **2019**, *9*, 5692–5697. [\[CrossRef\]](#)
- Shayegan, Z.; Haghighat, F. Effect of surface fluorination of P25-TiO<sub>2</sub> on adsorption of indoor environment volatile organic compounds. *Chem. Eng. J.* **2018**, *346*, 578–589. [\[CrossRef\]](#)
- Erdogan, N.; Jongee, P.; Woohyuk, C.; Soo, Y.K.; Abdullah, O. Alkaline hydrothermal synthesis, characterization, and photocatalytic activity of TiO<sub>2</sub> nanostructures: The effect of initial TiO<sub>2</sub> phase. *J. Nanosci. Nanotechnol.* **2019**, *19*, 1511–1519. [\[CrossRef\]](#) [\[PubMed\]](#)
- Gao, X.X.; Ge, Q.Q.; Xue, D.J.; Ding, J.; Ma, J.Y. Tuning the fermi-level of TiO<sub>2</sub> mesoporous layer by lanthanum doping towards efficient perovskite solar cells. *Nanoscale* **2016**, *8*, 16881–16885. [\[CrossRef\]](#) [\[PubMed\]](#)
- Giannakopoulou, T.; Papailias, I.; Todorova, N.; Boukos, N.; Liu, Y.; Yu, J.; Trapalis, C. Tailoring the energy band gap and edged potentials of g-C<sub>3</sub>N<sub>4</sub>/TiO<sub>2</sub> composite photocatalysts for NO<sub>x</sub> removal. *Chem. Eng. J.* **2017**, *310*, 571–580. [\[CrossRef\]](#)
- Lopez, R.; Ricardo, G. Band-gap energy estimation from diffuse reflectance measurements on sol-gel and commercial TiO<sub>2</sub>: A comparative study. *J. Sol-Gel Sci. Technol.* **2012**, *61*, 1–7. [\[CrossRef\]](#)
- Mara, M.W.; Bowman, D.N.; Buyukcakil, O.; Shelby, M.L. Electron injection from copper diimine sensitizers into TiO<sub>2</sub>: Structural effects and their implications for solar energy conversion devices. *J. Am. Chem. Soc.* **2015**, *137*, 9670–9684. [\[CrossRef\]](#)
- Ovsyannikov, S.V.; Xiang, W.; Vladimir, V.S.; Alexander, E.K.; Natalia, D.; Gaston, G.; Leonid, D. Structural stability of a golden semiconducting orthorhombic polymorph of Ti<sub>2</sub>O<sub>3</sub> under high pressures and high temperatures. *J. Phys. Condens. Matter* **2010**, *22*, 375402–375411. [\[CrossRef\]](#)
- Panayotov, D.A.; John, T.Y.J. Depletion of conduction band electrons in TiO<sub>2</sub> by water chemisorptions-IR spectroscopic studies of the independence of Ti-OH frequencies on electron concentration. *Chem. Phys. Lett.* **2005**, *410*, 11–17. [\[CrossRef\]](#)
- Qiu, M.; Yuan, T.; Zhangxian, C.; Zeheng, Y.; Wenming, L.; Kai, W.; Lei, W.; Kun, W.; Weixin, Z. Synthesis of Ti<sup>3+</sup> self-doped TiO<sub>2</sub> nanocrystals based on Le Chatelier's principle and their application in solar light photocatalysis. *RSC Adv.* **2016**, *6*, 74376–74383. [\[CrossRef\]](#)
- Lee, J.W.; Jeong, R.H.; Kim, D.I.; Yu, J.-H.; Nam, S.-H.; Boo, J.-H. Facile synthesis of amorphous Ti-peroxo complex for photocatalytic activity under visible-light irradiation. *J. Clean. Prod.* **2019**, *239*, 118013. [\[CrossRef\]](#)
- Gligorovski, S.; Strekowski, R.; Barbati, S.; Vione, D. Environmental implications of hydroxyl radicals. *Chem. Rev.* **2015**, *115*, 13051–13092. [\[CrossRef\]](#)

23. Shu, Y.; Ji, J.; Zhou, M.; Liang, S.; Xie, Q.; Li, S.; Liu, B.; Deng, J.; Cao, J.; Liu, S.; et al. Selective photocatalytic oxidation of gaseous ammonia at ppb level over Pt and F modified TiO<sub>2</sub>. *Appl. Catal. B Environ.* **2022**, *300*, 120688. [[CrossRef](#)]
24. Karmakar, S.; Barman, S.; Rahimi, F.A.; Biswas, S.; Nath, S.; Maji, T.K. Developing post-modified Ce-MOF as a photocatalyst: A detail mechanistic insight into CO<sub>2</sub> reduction toward selective C2 product formation. *Energy Environ. Sci.* **2023**, *16*, 2187–2198. [[CrossRef](#)]
25. Talaiekhosani, A.; Rezani, S.; Kim, K.-H.; Sanaye, R.; Amanie, A.M. Recent advances in photocatalytic removal of organic and inorganic pollutants in air. *J. Clean. Prod.* **2021**, *278*, 123895. [[CrossRef](#)]
26. Papailias, I.; Todorova, N.; Giannakopoulou, T.; Dvoranová, D.; Brezová, V.; Dimotikali, D.; Trapalis, C. Selective removal of organic and inorganic air pollutants by adjusting the g-C<sub>3</sub>N<sub>4</sub>/TiO<sub>2</sub> ratio. *Catal. Today* **2021**, *361*, 37–42. [[CrossRef](#)]
27. Zheng, W.; Liu, X.; Yan, Z.; Zhu, L. Ionic liquid-assisted synthesis of large-scale TiO<sub>2</sub> nanoparticles with controllable phase by hydrolysis of TiCl<sub>4</sub>. *ACS Nano* **2009**, *3*, 115–122. [[CrossRef](#)]

**Disclaimer/Publisher's Note:** The statements, opinions and data contained in all publications are solely those of the individual author(s) and contributor(s) and not of MDPI and/or the editor(s). MDPI and/or the editor(s) disclaim responsibility for any injury to people or property resulting from any ideas, methods, instructions or products referred to in the content.